

INTENSITY EFFECTS IN A CHAIN OF MUON RCSs

F. Batsch^{*,1}, H. Damerou¹, I. Karpov¹,
 D. Amorim¹, A. Chancé², A. Grudiev¹, E. Métral¹, D. Schulte¹, S. Udongwo³
¹CERN, Geneva, Switzerland
²CEA, Paris-Saclay, France
³University of Rostock, Germany

Abstract

The muon collider offers an attractive path to a compact, multi-TeV lepton collider. However, the short muon lifetime leads to stringent requirements on the fast energy increase. While extreme energy gains in the order of several GeV per turn are crucial for a high elevated muon survival rate, ultra-short and intense bunches are needed to achieve large luminosity. The longitudinal beam dynamics of a chain of rapid cycling synchrotrons (RCS) for acceleration from around 60 GeV to several TeV is being investigated in the framework of the International Muon Collider Collaboration. Each RCS must have a distributed radio-frequency (RF) system with several hundred RF stations to establish stable synchrotron motion. In this contribution, the beam-induced voltage in each RCS is studied, assuming a single high-intensity bunch per beam in each direction and ILC-like 1.3 GHz accelerating structures. The impact of single- and multi-turn wakefields on longitudinal stability and RF power requirements is analysed with particle tracking simulations. Special attention is moreover paid to the beam power deposited into the higher-order modes of the RF cavities.

INTRODUCTION

The recent improvements in accelerator technologies like superconducting magnets with fields beyond 8 T or high-gradient radio-frequency (RF) structures led to a strong interest in the development of a muon collider facility in the multi-TeV regime. The International Muon Collider Collaboration (IMCC) works towards a design proposal for a staged facility with 3 TeV to 10 TeV collision energy [1, 2] based on the US Muon Acceleration Program (MAP) [3, 4]. Luminosities of $2 \cdot 10^{35} \text{ cm}^{-2} \text{ s}^{-1}$ (at 10 TeV) are reached by colliding single high-intensity μ^+ and μ^- bunches with populations of $1.8 \cdot 10^{12}$ muons per bunch at the time of injection into the collider ring. The muon bunches are formed by depositing protons on a target, followed by 6-dimensional cooling. The subsequent accelerator complex consists of a low-energy part for an initial acceleration to an energy of about 60 GeV, and a high-energy part on which this paper focuses. A chain of rapid cycling synchrotrons (RCS) is foreseen to accelerate two counter-rotating bunches in stages of 0.30 TeV, 0.75 TeV and 1.5 TeV to finally 5 TeV at a repetition rate of 5 Hz, before injecting them into the separate collider ring. The accelerator chain is sketched in Fig. 1.

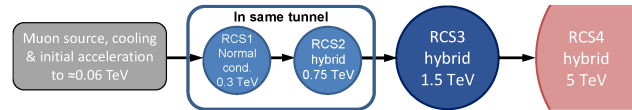


Figure 1: Schematic of the chain of rapid cycling-synchrotrons for the high-energy acceleration complex.

This design is fully driven by the muon decay. The muon lifetime at rest of $\tau_\mu = 2.2 \mu\text{s}$ is time-dilated by the extremely fast acceleration which extends the lifetime by the relativistic Lorentz factor γ , which reaches $4.7 \cdot 10^4$ at an energy of 5 TeV. A further challenge besides the fast acceleration is the high bunch population. Around $2.7 \cdot 10^{12}$ muons per bunch at the beginning of the RCS chain have to be accelerated to meet the target beam parameters [2] in the collider. Strong transient beam loading is expected due to the large peak current. For the studies, we extended the longitudinal macro-particle tracking code BLoND [5, 6] to the regime of multi-turn wakefields in multiple RF stations per ring. We observe the impact of these intensity effects on the longitudinal stability and the resulting RF power requirements. Single- and multi-turn wakefields are analyzed for the single bunches. We cover both the fundamental mode (FM) and higher-order modes (HOMs) of the RF cavities, including the beam power deposited into these HOMs.

BEAM AND RF PARAMETERS

A selection of preliminary parameters for the RCSs is listed in Table 1. Since the different RCSs are foreseen to use the same cavity type, our studies focus on the first RCS where the bunch population is highest. The RCS1 and RCS2

Table 1: Example parameters for the muon RCSs assuming a 90% survival rate per RCS and an RF system at 1.3 GHz. Values for RCS4 are draft parameters.

	RCS1	RCS2	RCS3	RCS4
Circumference [m]	5990	5990	10700	35000
Injection energy [TeV]	0.06	0.30	0.75	1.50
Ejection energy [TeV]	0.30	0.75	1.50	5.00
Acceleration time [ms]	0.34	1.10	2.37	6.4
Revolution period [μs]	20.0	20.0	35.7	117
Number of turns	17	55	66	55
ΔE per turn [GeV]	14.8	7.9	11.4	64
Bunch intensity [10^{12}]	2.7	2.43	2.2	2.0
Bunch length [1σ , ps]	<45	<33	<28	<17
Bunch current [mA]	21.7	19.5	9.9	3.0
Target ε_L (4σ) [eVs]	0.31	0.31	0.31	0.31

* fabian.batsch@cern.ch

are supposed to share the same tunnel as they have the same circumference and layout [7]. The bending in the first RCS is provided by normal conducting magnets. The RCS2 to RCS4 are planned as hybrid RCSs where normal conducting magnets cycling from $-B_{nc}$ to $+B_{nc}$ are interleaved with strong fixed-field, superconducting magnets.

Beam Parameters

The bunch populations for both μ^+ or μ^- are between $2.7 \cdot 10^{12}$ in RCS1 and $1.8 \cdot 10^{12}$ in RCS4. For each RCS, a decay loss of 10 % per RCS is presently assumed, even though these values have yet to be adjusted to optimize the RF parameters and bunch matching at a later stage. In the tracking code, a randomized deletion of particles according to their time-dilated decay rate ($\propto 1 - \exp[-\Delta t / (\tau_\mu \gamma)]$) per time step Δt is implemented to include the effect of decreasing beam intensities. The target bunch length at 1.5 TeV is only $1\sigma_z = 5$ mm, with a normalized longitudinal target 4σ emittance of $\varepsilon_L = 0.31$ eVs [2]. The line density λ of the muon bunch can be described by [8]

$$\lambda(t) = \lambda_0 \left[1 - \left(\frac{t}{\tau_l} \right)^2 \right]^\nu, \quad (1)$$

where ν defines the bunch shape and τ_l represents the full width at half maximum (FWHM) bunch length. A parabolic bunch is e.g. described by $\nu = 1$. For $\nu = 0.5$, one obtains a bunch where $\tau_l = 4\sigma_{rms}$. For the simulations, we generate a bunch such that τ_l corresponds to an emittance of $\varepsilon_L = 0.31$ eVs (4σ) and tails represent a longitudinal distribution with $\nu = 2.5$. This is motivated by the assumption that muons, due to the absence of synchrotron radiation due to the large mass, behave more like protons and not electrons.

RF System Parameters

The muon decay rate and the resulting strict gradient requirements [9] strongly impact the parameters of the RF system. Around 30 distributed RF stations are needed per RCS to reduce the otherwise excessive synchrotron tune between RF stations for stable synchrotron oscillations and phase focusing. For given injection and ejection energies and for a fixed survival rate of 90 %, the acceleration times τ_{acc} and average accelerating gradients G_{acc} that must be supplied along the full circumference of each RCS (including areas without RF) are fully determined. The acceleration times range from 0.3 ms to 6.4 ms (Table 1). Assuming a constant energy gain ΔE per turn (Table 1), the corresponding average gradients are $G_{acc} = 2.4$ MV/m, 1.3 MV/m, 1.1 MV/m and 1.8 MV/m, respectively. Together with the strong impact of intensity effects, high-gradient superconducting structures must be used. An ILC-like 1.3 GHz cavity, also known as TESLA cavity [10], is designed for high bunch charges and gradients and therefore selected to be tested in simulations. The cavity has nine cells, a length of 1.0 m and a geometry factor R/Q of 511Ω . For a synchronous phase of up to $\phi_s = 45^\circ$ and the energy gains per turn ΔE of Table 1, the installed RF voltages $V_{RF} = \Delta E / \cos(\phi_s)$ in RCS1 to RCS4

are respectively 20.9 GV, 11.2 GV, 16.1 GV and 90 GV at least. A maximum cavity voltage of 30 MV [10] (and thus an accelerating gradient of 30 MV/m) translates to 700 (RCS1), 380 (RCS2), 540 (RCS3) and 3000 (RCS4) cavities.

BEAM-INDUCED VOLTAGES

For single-turn intensity effects, the beam-induced voltage can be obtained by determining the short-range (SR) and FM beam loading contributions separately, as shown in [9]. The SR wakefields, which include the information of all HOMs, are computed according to the theory of K. Bane [11]. The longitudinal wake function $W_{L,SR}$ is approximated for bunch lengths much smaller than the cavity cell length L , i.e., for $\sigma_z/L < 0.1$. The contribution of the FM is computed using a resonator model [5], with resonator frequency $f_{RF} = 1.298$ GHz (at an integer harmonic of the revolution frequency), loaded quality factor Q_L ($Q_{L,0} = 2 \cdot 10^6$ for steady-state beam loading compensation [12]), and the shunt impedance (calculated from R/Q and Q_L) as input. However, for the muon bunches with $\sigma_z \leq 13$ mm, and 115 mm long cells, the condition $\sigma_z/L < 0.1$ is not always fulfilled.

Therefore, we describe the wakefields more accurately with the possibility to include multi-turn effects by calculating both FM and HOMs through a resonator model and then summing the individual induced voltage contributions. The information about HOMs is listed in literature [13, 14] but can also be obtained through simulations of the cavity structure with codes such as CST [15] or ABCI [16]. Figure 2 shows an example of the induced voltage in RCS1 (parameters from [13, 14] and Table 1) at injection (red), together with the charge line density $\lambda(t)$ (in arb. units, light-blue dotted) for a bunch length of $1\sigma_z = 13$ mm. For comparison,

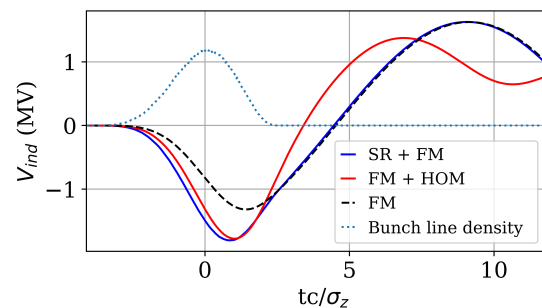


Figure 2: Normalized bunch charge density (light-blue dotted) and induced voltages per cavity in RCS1 versus time normalized to $1\sigma_z/c$. The voltages combining resonators for both FM (black dashed) and HOMs is shown in red, the sum of the FM and single-turn effects from SR wakefields from [9] in blue. Bunch center at time $t = 0$.

the contributions from the FM itself (black dashed line) and the voltage when the SR contribution according to [11] is added to the FM (blue solid) are also shown. Both induced voltages agree well in amplitude and position in the region of the bunch and reach almost 10 % of the cavity voltage without beam. The deviation for $tc/\sigma_z > 2$ is due to the long-range RF voltage induced into the HOMs.

LONGITUDINAL STABILITY

Previous studies [9] indicate that the effect of these single-turn wakefields does not excite instabilities. Here, we investigate the influence of the multi-turn wakefields of the HOMs. Their build-up from turn to turn strongly depends on the quality factor Q of each mode at angular frequency ω , as it is proportional to the cavity filling time $\tau_{\text{fill}} = 2Q/\omega$ and therefore to how fast the wakefields decay with respect to one revolution period. In other words, multi-turn effects contribute when the loaded quality factor is larger than the harmonic number of the RF system.

Preliminary results from tracking simulations investigating the effect of the quality factors of the HOMs on the longitudinal emittance are illustrated in Figs. 3 and 4. Figure 3 (a) shows the voltage induced into the HOMs accumulated over the in total 17 turns in RCS1, using the parameters from [13, 14] for a frequency range up to 6.7 GHz. For each mode, a quality factor in the range of $Q \approx 10^4$ is assumed. The voltages of up to 0.9 MV decay until the bunch

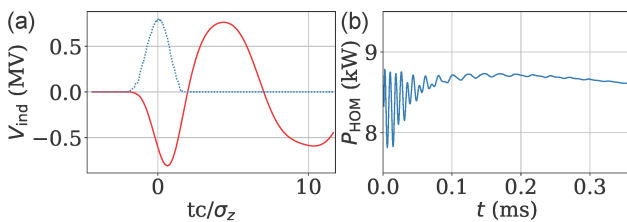


Figure 3: (a) Induced voltage into HOMs per cavity in RCS1 (red) and normalized bunch charge density (blue dotted) versus time normalized to $1\sigma_z/c$, bunch center at time $t = 0$. (b) RF power induced into HOMs versus time in RCS1.

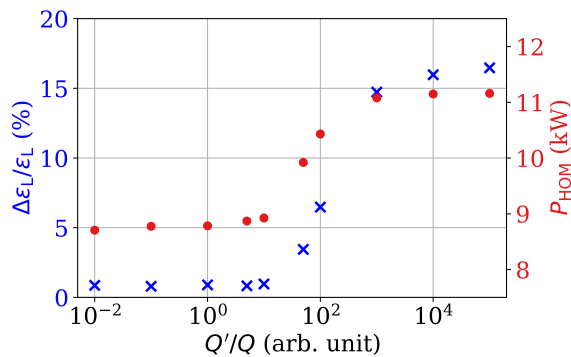


Figure 4: Left axis: Relative emittance growth at the end of the cycle with respect to the emittance at injection for various scaled quality factors Q' normalized to Q from [13, 14] (blue crosses). Right: HOM power losses versus Q'/Q (red dots).

passes again one revolution period later, and the relative longitudinal emittance growth due to the HOMs is small with $\Delta\varepsilon_L/\varepsilon_L \approx 1\%$.

To investigate the influence of the quality factor of the HOMs in view of a damping scheme design, we apply a factor to their original values. Factors Q'/Q between 10^{-2} and 10^5 are applied. In Fig. 4, the blue crosses represent the relative emittance growth $\Delta\varepsilon_L/\varepsilon_L$ versus Q'/Q . For

$Q'/Q \leq 10^1$, the emittance growths are around 1%. This growth increases significantly for $Q'/Q \geq 100$, where Q' roughly corresponds to the harmonic number of RCS1 (and RCS2) of $2.6 \cdot 10^5$. In this case, the decay time exceeds one revolution period, as expected.

BEAM-INDUCED POWER LOSSES

Of equal importance is the power induced into the HOMs. The average HOM power loss P_{HOM} per bunch during acceleration is calculated from the longitudinal wake function W_L as [17]

$$P_{\text{HOM}} = -k_{\parallel} \cdot \frac{q^2}{T_{\text{rev}}} ; k_{\parallel} = \int W_L(t) \cdot \lambda(t) dt, \quad (2)$$

with longitudinal loss factor k_{\parallel} , bunch charge q and revolution period T_{rev} that is equal to the bunch spacing. This wake function is simply obtained from the total induced multi-turn voltage due to HOMs. The induced power versus time in RCS1 for $Q'/Q = 1$ is depicted in Fig. 3 (b). Despite fluctuations because of an initial distribution mismatch, P_{HOM} stays relatively constant through the full acceleration cycle with a peak power of 8.8 kW, averaged over the acceleration time, which is in agreement with previous simulations [9]. Equivalent induced powers during the acceleration cycle for different Q' are plotted in Fig. 4 (red). With $Q'/Q \leq 10^1$, the peak power deposited in the HOMs remains at around 8.8 kW. For factors larger $Q'/Q = 10$ and consistent with the increasing emittance growths, the induced power builds up and values exceed 11 kW.

To handle these peak power losses, high-power HOM couplers with well defined quality factors will be required. It is important to keep in mind that P_{HOM} is averaged over the revolution period. The duty cycle is much lower because of the repetition rate of the 5 Hz, i.e., less than 1% for RCS1 to RCS3. For a design of high-power HOM couplers, the consequences of these large differences between peak power and CW limit have to be investigated.

CONCLUSION

Preliminary simulation results of the intensity effects during the acceleration of high-intensity muons in a chain of rapid-cycling synchrotrons for a future muon collision facility have been presented. High bunch populations up to $2.7 \cdot 10^{12}$ muons lead to strong transient beam loading. Induced voltages were calculated for single and multi-turn effects using a resonator model and are on the order of MV per cavity. The effect of multi-turn wakefields due to HOMs on the longitudinal stability is investigated and the power which is induced into these HOMs is studied as a function of their quality factors. Best results, with powers of around 9 kW, were obtained for quality factors scaled below 10^5 . Above, the emittance growth and induced power due to the HOMs increase. With the duty cycle being below 1%, the effect of these large powers on the CW limit of the HOM couplers is being investigated.

ACKNOWLEDGMENTS

The authors would like to thank Scott Berg, Rama Calaga, Leonard Thiele, and Ursula van Rienen for the fruitful discussions, support and helpful inputs during these studies.

Funded by the European Union (EU). Views and opinions expressed are however those of the authors only and do not necessarily reflect those of the EU or European Research Executive Agency (REA). Neither the EU nor the REA can be held responsible for them.

REFERENCES

- [1] C. Accettura *et al.*, “Towards a muon collider”, *Eur. Phys. J. C*, vol. 83, p. 864, 2023.
doi:10.1140/epjc/s10052-023-11889-x
- [2] D. Schulte *et al.*, “Bright Muon Beams and Muon Colliders”, CERN, Geneva, Switzerland, Rep. CERN-2022-001, European Strategy for Particle Physics - Accelerator R&D Roadmap, p. 145, 2022. doi:10.23731/CYRM-2022-001
- [3] M. A. Palmer, “Muon Accelerator Program (MAP)”, available online: <http://map.fnal.gov>
- [4] J. S. Berg, “Details and justifications for the MAP concept specification for acceleration above 63 GeV”, BNL, Upton, NY, USA, Rep. BNL-105415-2014-IR, 2014.
doi:10.2172/1149436
- [5] CERN Beam Longitudinal Dynamics code BLonD, <http://blond.web.cern.ch>
- [6] H. Timko *et al.*, “Beam longitudinal dynamics simulation studies”, *Phys. Rev. Accel. Beams*, to be published.
- [7] J. S. Berg, “Muon Collider Pulsed Synchrotron Parameters”, BNL, Upton, NY, USA, Rep. BNL-221336-2021-INRE, 2021.
doi:10.2172/1779395
- [8] J. L. Laclare, “Bunched beam coherent instabilities”, in *Proceedings of CAS 1985 vol. 1*, Oxford, UK, 1987, pp. 264–326.
doi:10.5170/CERN-1987-003-V-1.264
- [9] F. Batsch, *et al.*, “Longitudinal beam dynamics and RF requirements for a chain of muon RCSs”, in *Proc. 14th Int. Particle Accelerator Conf. (IPAC’23)*, Venice, Italy, May 2023, paper TUPA040, pp. 1428–1431.
doi:10.18429/JACoW-IPAC2023-TUPA040
- [10] B. Aune, “Superconducting TESLA Cavities”, *Phys. Rev. Spec. Top. Accel. Beams*, vol. 3, p. 092001, 2000.
doi:10.1103/PhysRevSTAB.3.092001
- [11] K. L. F. Bane *et al.*, “Calculations of the Short-Range Longitudinal Wakefields in the NLC Linac”, in *eConf C980914*, SLAC, CA, USA, SLAC-PUB-7862, 1998, pp. 137–139.
doi:10.2172/6431678
- [12] J. Tückmantel, “Cavity-Beam-Transmitter Interaction Formula Collection with Derivation”, CERN, Geneva, Switzerland, Rep. CERN-ATS-Note-2011-002 TECH, 2010.
- [13] R. Wanzenberg, “Monopole, Dipole and Quadrupole Passbands of the TESLA 9-cell Cavity”, DESY, Hamburg, Germany, Rep. DESY-TESLA-2001-33, 2001.
- [14] F. Marhauser, P. Huelsmann, and H. Klein, “Trapped Modes in TESLA Cavities”, in *Proc. PAC’99*, New York, NY, USA, Mar. 1999, paper FRA11, pp. 3405–3407.
doi:10.1109/PAC.1999.792318
- [15] CST Studio Suite, <https://www.3ds.com/products-services/simulia/products/cst-studio-suite>
- [16] ABCI, <https://abci.kek.jp/>
- [17] B. W. Zotter and S. Kheifets, “Loss Factors and Effective Impedances”, in *Impedances and Wakes in High Energy Particle Accelerators*, World Scientific, 1998.
doi:10.1142/9789812817389_0005